

Resonant photoemission study of superconducting Y-Ba-Cu-O

Richard L. Kurtz and Roger L. Stockbauer

Surface Science Division, National Bureau of Standards, Gaithersburg, Maryland 20899

Donald Mueller, Arnold Shih, Louis E. Toth,* Michael Osofsky, and Stuart A. Wolf

Naval Research Laboratory, Washington, D.C. 20375

(Received 15 April 1987)

Ultraviolet photoelectron spectra of a 93-K superconducting compound, $\text{YBa}_2\text{Cu}_3\text{O}_7$, have been obtained using photon energies ranging from 60 to 106 eV. Resonant photoemission is used to identify the chemical origin of the features in the valence-band electronic structure.

Recent developments in the production of high- T_c superconductors have spurred the rapid development of theories of the geometric and electronic structure of these compounds. A number of theoretical calculations of the band structures of La-Ba-Cu-O have been produced and studied in an effort to understand the nature of the superconducting process.¹ However, these calculations have not been supported by direct measurements of the band structures. With the production of the series of Y-Ba-Cu-O materials with critical temperatures above 77 K, measurements of the electronic structures below T_c have become experimentally more tractable.² An essential component of the interactions that produce the superconductivity is the electronic structure, yet measurements of this structure have not been made.

In this paper, we report the first measurements of the electronic structure of $\text{YBa}_2\text{Cu}_3\text{O}_7$ using synchrotron radiation in the range 60–106 eV. In this photon energy range, we are able to use resonant photoemission in order to assist in the chemical identification of the Cu and Ba features observed in the valence-band spectra. Resonant photoemission is associated with an enhancement of valence photoelectron features resulting from the coupling of excitation and decay mechanisms at core-electron photoabsorption onsets.

The samples of $\text{YBa}_2\text{Cu}_3\text{O}_7$ were prepared by mixing oxides and carbonates of the metals in the appropriate atomic ratios, and calcining in air. The samples were pressed into pellets and sintered in air and O_2 . The material is single phase and the structure is that determined by Beech, Miraglia, Santora, and Roth³ using neutron powder diffraction at the National Bureau of Standards. Four-point ac resistance measurements show a sharp drop in the resistance at 93 K and zero resistance is attained at 91 K.

The photoemission measurements were made using the National Bureau of Standards SURF-II synchrotron light source, a toroidal grating monochromator, and a double-pass cylindrical mirror analyzer (CMA). Base pressures were $\sim 1 \times 10^{-10}$ Torr. The sample normal was at an angle of 45° to both the photon beam and the axis of the analyzer; the spectra obtained are angle integrated. Calculated photon resolution is 350 meV at a photon energy of 60 eV. The CMA was operated with a constant pass energy giving a constant resolution of 240 meV; the data

are presented uncorrected for CMA transmission. Samples were mounted on a liquid-nitrogen-cooled manipulator using Ta foil and held into an Al ring with In in order to produce good thermal contact. The temperatures were measured with a W-5% Re, W-26% Re thermocouple imbedded in the In. The surfaces were prepared in ultrahigh vacuum by fracturing the microcrystalline needles with a stainless-steel blade. The Fermi level was determined from photoemission spectra of a clean gold foil that was in electrical contact with the sample. Measurements were made on two separate batches of oxide superconductor. Spectra from both samples showed the same features at identical binding energies; however, the second sample which had been sintered longer showed sharper peaks.

Figure 1 shows a survey of ultraviolet photoelectron spectra (UPS) from the first sample in the photon energy range 60–106 eV in 2-eV increments. At a photon energy of 60 eV (top curve), we observe primarily two valence-band features centered at binding energies of 5 and 9.4 eV. As the photon energy is increased, the 9.4-eV peak is enhanced slightly and an additional feature at 12.4 eV is observed. This peak rises to a maximum at a photon energy near 74 eV and then decays in intensity, along with a portion of the 9.4-eV feature. With increasing photon energy, two additional peaks become apparent, centered at binding energies of 15 and 28.8 eV. Over the photon energy range spanned by Fig. 1, several low-energy Auger features are also observed; they appear at constant *kinetic* energy, i.e., at 2 eV higher *binding* energy in successive curves.

Figure 2 shows, in more detail, photoemission spectra obtained from the second sample with photon energies of 74 and 94 eV, the resonant energy for Cu and an off resonance energy, respectively. The Ba resonance occurs at photon energies near 104 eV. The long dashed curves in Fig. 2 represent an approximation to the secondary electron contribution and the multiple features observed in these curves are fit using simple Gaussian line shapes. The detailed form of the secondary background does not, to first order, affect the locations or widths of the features but it can influence their intensities. Here, we are primarily interested in locating the energies of these features and this decomposition allows a better estimation.

The primary photoelectron feature (valence band), located immediately below E_F , contains at least two contri-

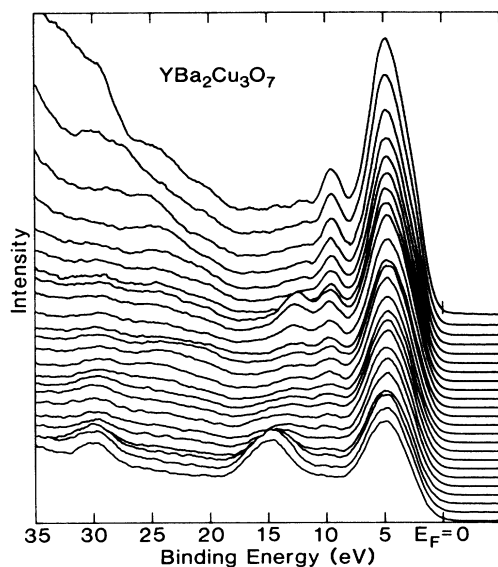


FIG. 1. Ultraviolet photoemission spectra obtained from ultrahigh vacuum fractured $\text{YBa}_2\text{Cu}_3\text{O}_7$. The top curve is obtained with $h\nu = 60$ eV and the lower curve is with $h\nu = 106$ eV; successive curves are separated by photon energy increments of 2 eV. These data were obtained from the first sample. The spectra obtained from the second sample are essentially identical.

butions that are centered at 2.3 and 4.5 eV. These states arise primarily from Cu 3d and O 2p orbitals. The upper edge of the valence band nearly coincides with the Fermi level and the density of states at E_F is small; there is no distinctive edge. This valence band is *not* observed to resonate with photon energy. The other O-related feature in the binding energy region shown in these spectra is the O 2s level, observed with a low cross section at a binding energy of 20.1 eV.

As indicated above, the intensities of several of the photoemission features are observed to resonate with the photon energy. This resonant enhancement is observed both for Cu 3d satellites and for Ba 5s and 5p levels. The Cu satellite resonant enhancement occurs as a result of an interference between an Auger process and a shake-up effect.⁴ This enhancement occurs at a photon energy of 74.2 eV in CuO and results in two satellites whose apparent binding energies are 12.9 and 10.5 eV with respect to the Fermi level.⁵ In Cu metal, the enhancement occurs at a photon energy of 75.6 eV and results in two satellites at 14.6 and 12.0 eV.⁵ In Cu_2O enhancement occurs at 76.5 eV and results in a single satellite at an apparent binding energy of 15.3 eV.⁵ The distinct behavior of the satellites for the different Cu oxides should allow us to identify its chemical state in the $\text{YBa}_2\text{Cu}_3\text{O}_7$ superconductor. In Fig. 2(a) the resonantly enhanced Cu satellites are observed at 12.4 and 9.4 eV, closest in energy to the satellites observed in CuO. The other distinguishing feature of CuO is the persistence of intensity in these satellites off resonance, as observed here [see Fig. 2(b)]. At this point, the presence of Cu^{3+} cannot be established, due to lack of information about its possible satellites.

To better characterize the photon energy dependence of

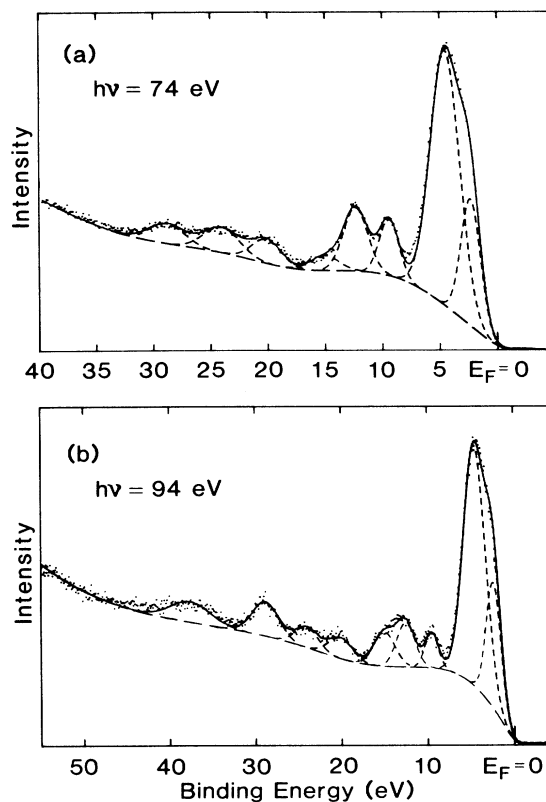


FIG. 2. Photoemission spectra obtained from the second sample for photon energies of 74 and 94 eV (data points are given by the dots). (a) is the resonant energy for Cu and (b) is off resonance. The background of secondary electrons is approximated by the long dashed curve and the features in the spectrum are decomposed into a sum of Gaussian peaks (short dashed curves). The sum of the Gaussian peaks and the secondary background give the solid curve.

the 12.4- and 9.4-eV satellites observed here, we have fit these features with Gaussian peaks as shown in Fig. 2, but in order to use consistent secondary electron approximations, a "Shirley method" background was used.⁶ This gives a reasonable approximation to the form of the secondary background for energies near E_F . Figure 3 shows the photon energy dependence of the two Cu satellites over the energies where resonance is expected. The scatter in the curves is within the precision of the intensity determinations. The enhancement of the 12.4-eV feature is much stronger than for the 9.4-eV feature; however, the latter feature contains an overlapping contribution that is most likely a multielectron feature that has been observed in photoemission from metallic Y.⁷ Both of these satellites are strongly enhanced at photon energies near 74.5 eV. Based on these observations, we assign the feature at 12.4 eV and a portion of the feature at 9.4 eV to resonantly enhanced satellites of Cu in a CuO-like oxide. The resonance energy is also in good agreement with that of CuO. At the lowest photon energies, the majority of the intensity of the 9.4-eV feature is likely to be due to Y.⁷ By comparison with ultraviolet photoemission spectroscopy from metallic Y, the feature at 24-eV binding energy is

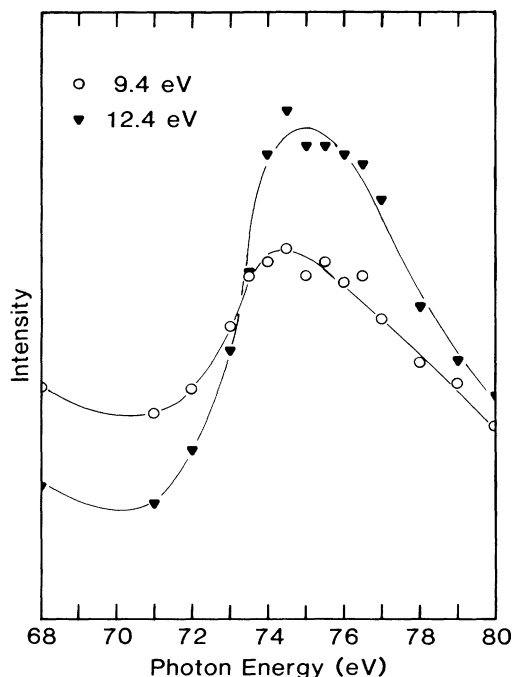


FIG. 3. Intensities of the 9.4- and 12.4-eV features vs photon energy. A smooth curve has been drawn through the points. The feature at 9.4 eV contains contributions from Y and from a Cu 3*d* satellite. The 12.4-eV feature is due to the second resonant Cu 3*d* satellite. The shapes and energy locations of these features are consistent with previous observations for the resonant behavior of CuO.

most likely due to the Y 4*p* level.

The apparent binding energies of the Cu satellites in the oxide superconductor are significantly lower than those in CuO. This may imply that the *d-d* Coulomb interaction U_{eff} for the Cu cation in this material is smaller than in CuO. From the information here, it may be possible to extract this U_{eff} ; however, the issue is more complex. It has been suggested that CuO is a charge-transfer semiconductor, where the bandgap is characterized by the charge-transfer energy Δ .⁸ Whether or not this may be the case for YBa₂Cu₃O₇ is unclear.

When the photon energy exceeds 94 eV, the features at 15.0 and 28.8 eV are observed to be resonantly enhanced. This enhancement may be due to an interference with the excitation of the Ba 4*d* levels [whose binding energies in BaO are 91 and 93.1 eV (Ref. 9)] and the two peaks are identified as Ba 5*p* and Ba 5*s* levels, respectively. This identification is confirmed by comparison of these valence

TABLE I. Binding energies (± 0.1 eV) referenced to E_F and full widths at half maximum (± 0.2 eV) of electronic energy levels of YBa₂Cu₃O₇ superconductor.

Level	Energy	FWHM
Cu 3 <i>d</i> /O 2 <i>p</i>	2.3	2.0
Cu 3 <i>d</i> /O 2 <i>p</i>	4.5	3.0
Y/Cu satellite	9.4	1.9
Cu satellite	12.4	2.5
Ba 5 <i>p</i>	15.0	2.9
O 2 <i>s</i>	20.1	3.3
Y 4 <i>p</i>	24.0	3.1
Ba 5 <i>s</i>	28.8	3.6

levels with x-ray photoelectron spectroscopy data from BaO.⁹ There, the Ba 5*p* level has a binding energy of 15.2 eV and the Ba 5*s* level is observed at 30.6 eV, essentially in agreement with the observations made here. Also observed in the spectrum shown in Fig. 2(b) is a feature located at an apparent binding energy of 37.6 eV. This is identified as a Ba *NVV* Auger electron feature. Table I presents a listing of the energies and identifications of the valence features observed in this study.

Within the resolution of this study, there is no evidence for valence-band structural changes associated with superconductivity as the temperature is lowered below T_c . In these measurements, the lowest temperatures attained were 88 K. There are other effects of operating at low temperatures, though, especially the increased sticking probability of H₂O. Even at 1×10^{-10} Torr, the contamination of the surface due to H₂O adsorption was observed over time periods as short as 30 min. This surface contamination is observed both as a reduction of the intensity of the 2.3-eV valence band and by the introduction of the 1*b*₂, 2*a*₁, and 1*b*₁ molecular orbitals.

In conclusion, we have measured the valence electronic structure of YBa₂Cu₃O₇ above and below the critical temperature. The valence-band edge is located immediately below the Fermi level; a sharp Fermi edge was not observed. The features observed in the spectra have been identified with the use of resonant photoemission. The Cu oxide in the superconducting material is similar to CuO, even though the characteristic Cu satellites observed here are located at lower energies. This result may have important implications about the nature of the charge-transfer process.

R.L.K. and R.L.S. wish to acknowledge discussions with Steven Girvin and support from the U. S. Office of Naval Research.

*Permanent address: National Science Foundation, Washington, DC 20375.

¹L. F. Mattheiss, Phys. Rev. Lett. **58**, 1028 (1987); J. Yu, A. J. Freeman, and J.-H. Xu, *ibid.* **58**, 1035 (1987); J. D. Jorgensen *et al.*, *ibid.* **58**, 1024 (1987).

²M. K. Wu, J. R. Ashburn, C. J. Torng, P. H. Hor, R. L. Meng, L. Gao, J. Huang, Y. Q. Wong, and C. W. Chu, Phys. Rev. Lett. **58**, 908 (1987).

³F. Beech, S. Miraglia, A. Santora, and R. S. Roth, Phys. Rev. B (to be published).

⁴M. Iwan, F. J. Himpsel, and D. E. Eastman, Phys. Rev. Lett. **43**, 1829 (1979).

⁵M. R. Thuler, R. L. Benbow, and Z. Hurych, Phys. Rev. B **26**, 669 (1982).

⁶D. A. Shirley, Phys. Rev. B **5**, 4709 (1972).

⁷S. D. Barrett and R. G. Jordan, Z. Phys. B (to be published).

⁸J. Zaanen, G. A. Sawatzky, and J. W. Allen, Phys. Rev. Lett. **55**, 418 (1985).

⁹R. E. Thomas, A. Shih, and G. A. Haas, Surf. Sci. **75**, 239 (1978).